# A NEW INTEGRATED AC-DC CONVERTER FED SENSORLESS CONTROLLING TECHNIQUE FOR A 3-PHASE BLDC MOTOR

RAJESH NALLI*, SUBBARAO K. , RAMAMOORTHI, KIRANKUMAR M.

Department of EEE, Koneru Lakshmaiah Education Foundation, Vaddeswaram, AP, India
*Corresponding Author: rajeshnalli123@kluniversity.in

## Abstract

This paper deals with a new power factor correction based $ib^3$ converter fed sensorless BLDC motor controlling technique. New flux linkage based sensorless control technique for a 3-phase BLDC motor has been proposed. A brief introduction to the conventional sensorless techniques like Back emf detection of floating phase, free-wheeling diode detection technique, back emf third harmonic detection techniques are discussed as well. Since the conventional sensorless technique has drawbacks like high frequency noise; more switching losses in free-wheeling diode detection methods (this method requires a number of additional switches). Wrong estimation of rotor position in back emf zero detection technique at low speeds where the floating phase back emf is considered for commutation instant estimation. In all the above discussed methods the back emf estimation is a speed dependent function, whereas in the proposed controlling technique the flux linkage calculation is not a speed ($\omega$) dependent function. Hence, the accuracy of rotor position prediction will be better than conventional methods. The analysis of the proposed technique is compared with conventional sensor based controlling techniques to validate the accuracy. The proposed technique is implemented using MATLAB/SIMULINK software.

Keywords: 3-$\phi$ BLDC motor, Flux linkage algorithm, High speed applications, Integrated AC-DC converter, Sensorless controlling technique.

## 1.  Introduction

It has become a general trend till recent times for most of the industries to adopt induction and DC motors for drive applications. But from the past two decades the BLDC motor became the most preferable choice in drive applications. Because it has a high torque to weight ratio like an induction motor drive and has very smooth speed control like a DC motor drive. In addition to this BLDC motor is robust and simple in fabrication. The great advantage of BLDC motors is its speed control. Speed of the motor can be controlled by power electronic switches (i.e., IGBT's, SCR's). Due to these characteristic features, the BLDC motor became the top priority motors in domestic and industrial applications.

Construction-wise BLDC motor has a stator which carries stator winding and a rotating permanent magnet of alloy material placed inside the stator frame called a rotor. BLDC motor rotation is controlled through switching of inverter switches on the stator side. This inverter switching function is based on the feedback signal of rotor position. To get the rotor position information BLDC motors conventionally uses hall-effect sensors. Hall sensors are mounted on the stator frame of the BLDC motor. The output voltage of the sensors is proportional to the applied magnetic field strength.

The sensor based controlling techniques fail in few areas like petroleum and mining industries, where these magnetic sensors may cause flaming inside the motor. To overcome this drawback sensorless techniques are adopted. Sensorless controlling techniques are classified as back emf detection, back emf integration, back emf's third harmonic integration and freewheeling diode conduction [1, 2].

In every technique there is a definite advantage and disadvantage. Details of these techniques are discussed in this paper. The back emf detection method [3] has limitations of speed range and floating neutral phase shifting. The back emf zero crossing time [4] always suffers with noise of high frequency distortion. Jang et al. [5] proposed the position detection of the rotor by inductance variation.

Singh and Singh [6] discussed the state of art on PM brushless drive controllers. Biswas et al. [7] proposed field oriented speed controlling using an adaptive controller. The rotor position detection by speed independent G($\theta$) function is discussed by Kim and Ehsani [8]. Based on estimated and actual detected state variables, the motor controlling method is proposed by Matsui [9].

All the conventional sensorless techniques have drawbacks like wrong estimation of rotor position, requirement of additional filters usage, requirement of additional switches. By adopting these techniques there is an increase in the power loss. The history of existing sensorless controlling techniques explained by Nalli et al. [10]. Nagi et al. [11, 12] and Sivani et al. [13] discussed the Dc to Dc converter topologies. The AC-DC converter dynamic behaviour is explained in [14]. Ahmad et al. [15] proposed the sensorless control of brushless DC motor by zero crossing detection generation with adaptive power factor control technique [15] cannot work accurately at low speed. Awchar et al. [16] discussed Advanced techniques for speed control of sensorless BLDC motors.

To overcome the drawbacks of all conventional controlling techniques we are proposing the flux linkage based rotor position estimation and an integrated AC-DC converter as front end converter.

## 2.    Modelling of Brushless DC Motor

A 3-phase BLDC motor mathematically modelled with the help of following expressions:

$V_{ac}., V_{bc}., V_{ba}$= voltage between two phases,

$I_a., I_b., I_c$ = phase currents passing in 3-phase windings,

$R_a = R_b = R_c = R$ = Resistances of each phase in ohm's,

$L_{as}, L_{bs}, L_{cs}$ = self-inductance in milli-henry,

$e_{ac}, e_{bc}, e_{ba}$ = back emf induced between two phases.

$L_{as} + L_m = L$   Where L is the inductance at circuit balanced condition

Voltages across each phase are:

$$V_a = i_a R + L \frac{di_a}{dt} + e_a$$
$$V_b = i_b R + L \frac{di_b}{dt} + e_b \tag{1}$$
$$V_c = i_c R + L \frac{di_c}{dt} + e_c$$

Induced 3-$\phi$ back Emfs  are.

$$e_a = K_e.f(\theta_a).\omega$$
$$e_b = K_e.f(\theta_b).\omega \tag{2}$$
$$e_c = K_e.f(\theta_c).\omega$$

In a balanced electric circuit, the resistance and self-inductance of three phases are the same and equal to 'R' and (L). In a 3-phase system the line or phase to phase voltages are expressed mathematically using Eqs. (3) and (4).

$$V_{ac} = R (i_a - i_c) + L \, d \, (i_a - i_c)/dt + e_{ac} \tag{3}$$

$$V_{cb} = R (i_c - i_b) + L \, d \, (i_c - i_b)/dt + e_{cb} \tag{4}$$

Here the mutual inductance between any two phases is constant, hence it is not considered.

According to KCL law the algebraic summation of currents is zero at a considered node expressed as.

$$i_a + i_b + i_c = 0 \tag{5}$$

Current passing through Phase C is.

$$i_c = -i_a - i_b \tag{6}$$

(For two phase operations when phases *a* and *b* conduct, phase c is open and $I_c$=0).

By solving Eqs. (3), (4) and (6) the current passing through phases A $(i_a)$ *and phase B*$( i_b)$ obtained as

$$i_a = \int \frac{2}{3L} V_{ac} + \frac{1}{3L} V_{cb} - \frac{1}{L} i_a R - \frac{2}{3L} e_{ac} - \frac{1}{3L} e_{cb} \tag{7}$$
$$i_b = \int -\frac{1}{3L} V_{ac} - \frac{2}{3L} V_{cb} - \frac{1}{L} i_b R + \frac{1}{3L} e_{ac} + \frac{2}{3L} e_{cb} \tag{8}$$

The electromagnetic Torque $(T_e)$ can be expressed using equation

$$T_e = k_t[(f(\theta_a)I_a) + (f(\theta_b)I_b) + (f(\theta_c)I_c)] \tag{9}$$

where $k_t$ is electromagnetic torque constant. Let first order equation expressed in mechanical equivalents as

$$J\frac{d\omega_m}{dt} + B\omega_m = T_e - T_L \qquad (10)$$

From Eq. (10) the angular speed of rotor is defined as

$$\omega_r = \frac{T_e - T_L}{Js + B} \qquad (11)$$

## Operating modes of proposed technique

The phase current ($I_{ph}$) flowing through stator winding of the Brushless DC motor is controlled by triggering the 3-phase inverter switches in sequential manner. The 3-phase inverter switches are named as $S_1$ to $S_6$ (shown in Fig. 1).
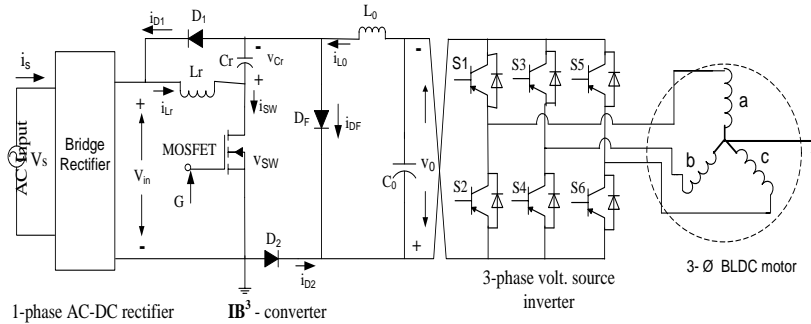


**Fig. 1. Configuration of 3-PhaseBLDC motor drive
with IB$^3$ (DC-DC Converter) as Front End converter.**

The initiation of switches conduction pattern takes place only, after monitoring the rotor position (i.e., stator pole phase to rotor pole phase alignment of a BLDC motor at steady position). To bring this alignment a short DC pulse is applied to one of the three phases.

When the phase voltage passes through stator winding the electromagnetic field developed by the stator phase attracts the rotor pole of the BLDC motor. The magnetic locking between stator poles to rotor poles takes place here since the magnetic flux always tries to flow through a low reluctance path. By this way the rotor position of the motor can be estimated (Fig. 2).
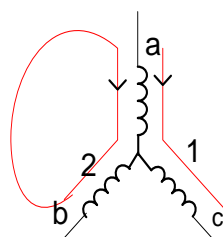


**Fig. 2. Conducting and free -wheeling paths.**

Once the rotor position of the drive is estimated the next conduction sequence is controlled using an FPGA controller. Spartan6 based PWM controller is used in

the proposal. The switching frequencies of IGBTS are 50 kHz. The conduction sequence of the proposed algorithm is shown in Table 1.

The developed flux linkages of 3-phase machines are triangular in shape under ideal condition which is shown in Fig. A-1 (*Appendix A*). The current conduction paths of stator phases are followed as a-c., b-c., b-a.

These combinations are excited sequentially one after another. Switching patterns of this technique are taken as $S_1$-$S_6$, $S_3$-$S_6$, $S_3$-$S_2$, $S_5$-$S_2$, $S_5$-$S_4$, $S_1$-$S_4$. Conduction flow of mode-1 is $+V_{dc}$-$S_1$-a-c-$S_6$- $-V_{dc}$ as shown in Fig. 3, it is freewheeling path is b-$D_3$-$S_1$-a. which is shown in Fig. 4. The expressions for phase currents derived in Eqs. (14), (15) and Eq. (16). The list of design components and its ratings of a BLDC motor are provided in Table A-1 (*Appendix A*).

Conducting path (1):

$$V_{dc} - i_1 2R - 2i_1 Ls - e_a - e_c = 0 \qquad\qquad 12(a)$$
$$i_1 = V_{dc} - e_a - \frac{e_c}{2(R+Ls)} \qquad\qquad 12(b)$$

Freewheeling path (2)

$$i_2 2R - 2i_2 Ls + e_b + e_a = 0 \quad i_2 = -(e_b + e_a)/2(R + Ls) \quad \} \qquad (13)$$

Here "S" is Laplace operator

$$i_a = i_1 + i_2 \qquad\qquad (14)$$
$$i_b = i_2 \qquad\qquad (15)$$
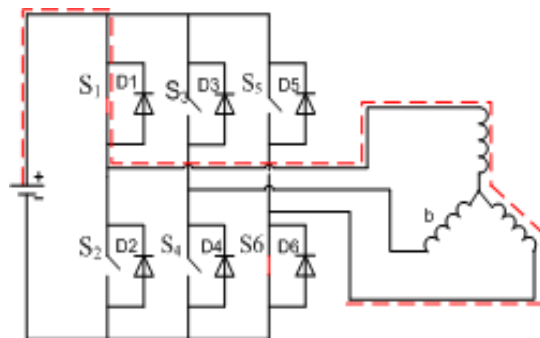$$i_c = i_1 \qquad\qquad (16)$$



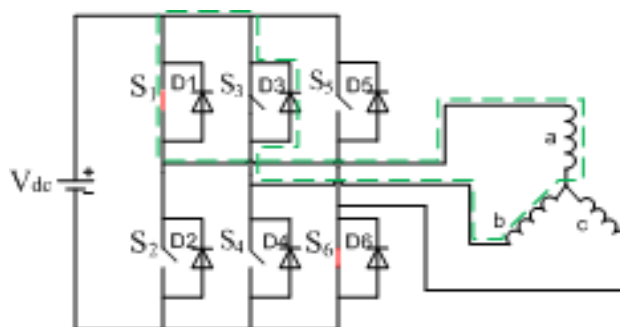**Fig. 3. Line current conduction path during switches 1,6 are ON.**



**Fig. 4. Free-wheeling path between A, B phases.**

Mathematically line Voltages and phase currents are taken for back-emf calculation. The expression for back-emf is $E = V - IR - L\frac{di}{dt}$. On other hand the induced emf is the rate of change of flux linkage, i.e., $E = \frac{d\varphi}{dt}$. This is the fundamental expression for E. From the available E.M.F. the flux linkages can be obtained by integrating E. The expression for flux linkages ($\varphi$) is defined in Eq. (17).

$$\varphi = \int V_L - 2I_a R_a - 2L\frac{di_a}{dt} \tag{17}$$

## 3.  Control Technique of Proposed Method

The controlling circuit contains the basic functional blocks of the proposed technique (Fig. 5). Two PI controllers used, one is one is responsible for converters closed loop operation, which is located near to the DC-DC converter block. The other PI controller responsible for motors closed loop operation, AC-DC converter, VSI, IGBTS are used for inverter switches, DSP controller and a three-phase BLDC motor.
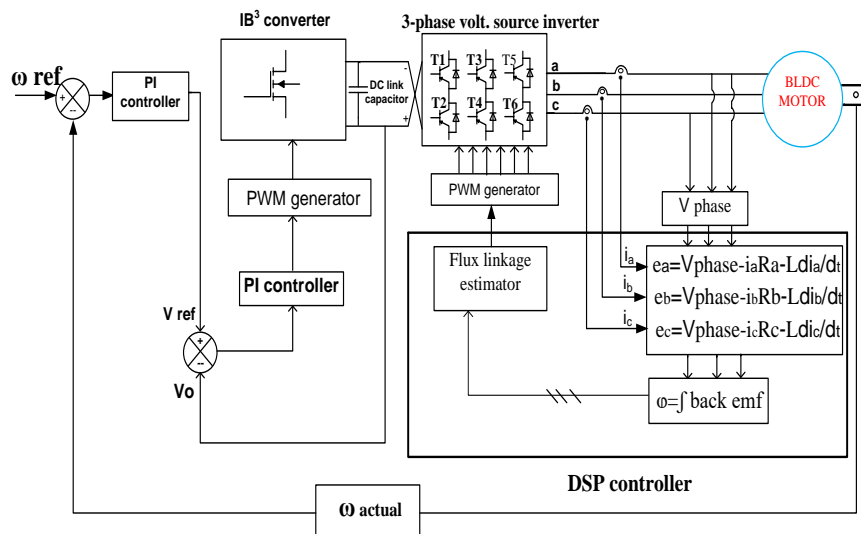


**Fig. 5. Control circuit diagram of proposed technique.**

### 3.1. PI speed controller design

The proposed method uses two stages PI controllers stage1. Converter pi controller: This controller used for AC-DC boost converter performance improvement purpose. Stage 2. Motors PI controller: this controller is used to get fast and accurate response characteristics of 3-phase BLDC drive. The functions of PI controllers are described as: The proportional part reduces the disturbance from the plant. Whereas the integral part reduces steady state error in the system [17].

The proportional part is proportional to error:

$$U = K_P e(t) \tag{18}$$

Integral part will be proportional to area under error curve:

$$U = K_I * \int_0^t e(\tau)d\tau \tag{19}$$

PI controller algorithm can be implemented as

$$U(t) = K_p e(t) + K_I \int_0^t e(\tau) d\tau \qquad (20)$$

where $e(t)$ = set reference value – actual calculated

**i. Inner PI controller (Converter side):**

After various approaches for tuning parameters of PI controller, the suitable gain values of $K_p, K_I$ are $K_p=$ and $K_I = 15$. The initial tuning values are taken from [14], Performance and Dynamic Analysis of Single Switch AC-DC Buck-Boost Buck Converter. The gain values are tuned manually for the inner PI controller.

**ii.  Outer PI controller:**

The gain values are tuned in such a way that it provides linear variation for the speed, the auto tuning would provide the best gain values once the motor starts rotating. $Kp$ and $K_I$ values are designed from the BL DC Motor controller design. Equations (18)-(20) describe the formulations required to calculate the error values.

### 3.2. Speed control of the BLDC motor

The error $e(t)$ value is obtained from its reference $\omega(ref)$ value and the actual speed of motor $\omega(\text{actual})$

$$e(t) = \omega(\text{ref}) - \omega(\text{actual})$$

The output of the pi controller is *Vref*. Conventionally the output of the pi controller is *Iref* always, since we are using the voltage model the output of the main pi controller is *Vref*. This *Vref* is compared with AC-DC converters output voltage (*Vdc*) , the resultant error sent to the inner pi controller to get the closed loop operation of the dc-dc converter.

### 3.3. Voltage and current sensor

The hardware implementation for the proposed technique can be done using a DSP control circuit (TMS320F28335) which operates at a maximum of 5 v DC range. Whereas the drive parameters work at high power ratings in order to drive the loads. In order to meet this requirement, voltage and current transducers are using These transducers sense the high voltage and currents and produce low voltage and current values which is suitable to controller particulars, the ADC's inside the hardware set up of DSP do all the arithmetic and logic functions, flip-flops work the protection circuits, the sensing gain values are adjusted to controller through programming.

The TMS320F28335 [18] takes the voltage and current values through input ports and performs all mathematical functions as described in the Eqs. (1) to (20). By this way the flux linkages developing inside the motor can be observed. Since the BLDC is a 120 phase displaced operating machine the next conducting sequence can predict accordingly PWM signals generated by the controller which are sent to the VSI inverter. The inverter is a IGBT based current controlled voltage source inverter (CC-VSI),where the switching frequency of the IGBT used in the VSI inverter is 20 kHz.

Switching sequences of 3-phase inverters based on magnitudes of phase flux linkages are given in Table 1.

**Table 1. switching states of 3-phase inverter.**

| Flux linkages of individual Phase (web-turns) | | | Switching sequence of six-switch Inverter | | | | | |
|---|---|---|---|---|---|---|---|---|
| $\psi_a$ | $\psi_b$ | $\psi_c$ | $S_1$ | $S_2$ | $S_3$ | $S_4$ | $S_5$ | $S_6$ |
| $> 0$ | $< 0$ | $> 0$ | ON | OFF | OFF | OFF | OFF | ON |
| $> 0$ | $< 0$ | $< 0$ | OFF | OFF | ON | OFF | OFF | ON |
| $> 0$ | $> 0$ | $< 0$ | OFF | ON | ON | OFF | OFF | OFF |
| $< 0$ | $> 0$ | $< 0$ | OFF | ON | OFF | OFF | ON | OFF |
| $< 0$ | $> 0$ | $> 0$ | OFF | OFF | OFF | ON | ON | OFF |
| $< 0$ | $< 0$ | $> 0$ | ON | OFF | OFF | ON | OFF | OFF |

Switches $S_1, S_3, S_5$ *and* $S_2, S_4, S_6$ are the upper and lower leg switches of 3-ϕ inverter.

### 3.4. Speed calculation

From the generalized state space equation of BLDC motor the back emf directly proportional to flux linkages explained in Eq. (21).

$$\begin{vmatrix} e_a \\ e_b \\ e_c \end{vmatrix} = \omega_m \lambda_m \begin{vmatrix} f_{as}(\theta_r) \\ f_{bs}(\theta_r) \\ f_{cs}(\theta_r) \end{vmatrix} \tag{21}$$

The electromagnetic toque

$$T_e = [e_a i_a + e_b i_b + e_c i_c]/\omega_m \tag{22}$$

From Eq. (22), the speed of the machine depends on back emf, i.e., indirectly depends on flux linkage [16, 19]. It may not depend on output frequency of DC-DC converter.

For small, rated BLDC motors the speed depends on constant like *Kv*, *Kt*, *Km*, based on its designed parameters, weight, number of coil turns, current flowing through winding, etc. Thereby small motors also run at thousands of rpm (example drone motors, hard disc drives, etc.).

### 4. Results and Discussions

Integrated buck boost buck (IB³) converter taken as front end converter for developing low ripple voltages for 3-phase inverter. The major advantage of this converter is the usage of single switch and having less filter components at DC side. Inside the motor the phase current waveforms are of Quasi square shape as shown in Figs. 6 to 8. This type of phase currents will produce high and constant torque while the motor is working.
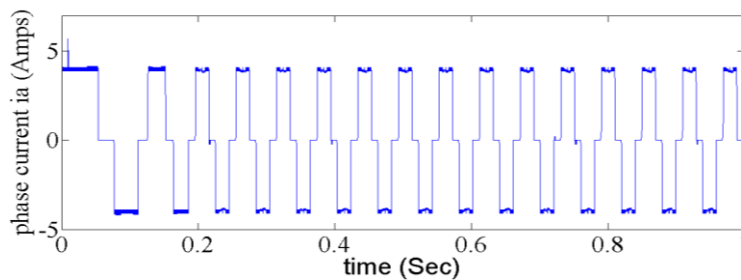


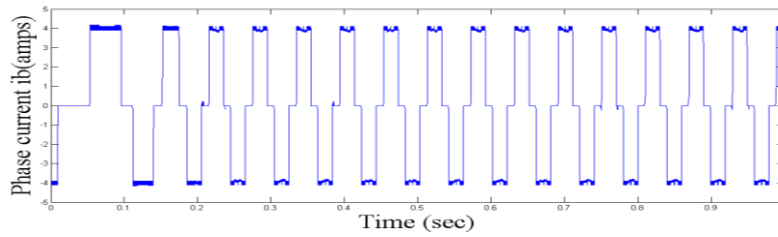**Fig. 6. Simulation value of phase A current waveform (amps).**

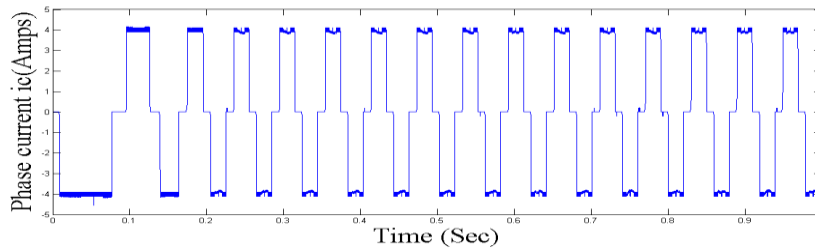**Fig. 7. Simulation value of phase B current wave form (amps).**



**Fig. 8. Simulation value of phase C currents wave form (amps).**

The expressions for Line voltages $v_{ac}$ and $v_{bc}$ are derived in Eqs. (3) and (4) which are shown in Figs. 9 and 10. Flux linkages which are triangular in shape are obtained by integrating the back emf of each phase as shown in Fig. 11. The developed phase back emf's are trapezoidal in shape as shown in Figs. 12 to 14. The outcome of results shown in Figs. 12 to 14 explains the combined effect of phase currents, back emf and flux linkages.
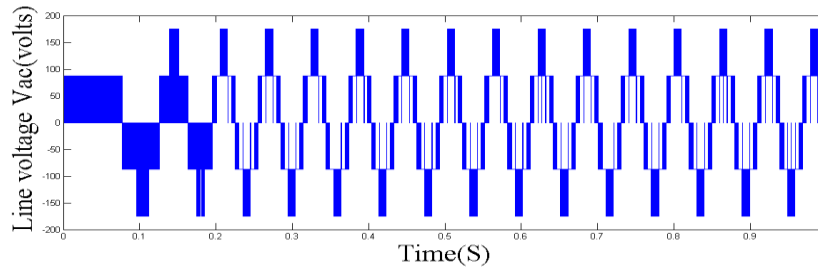


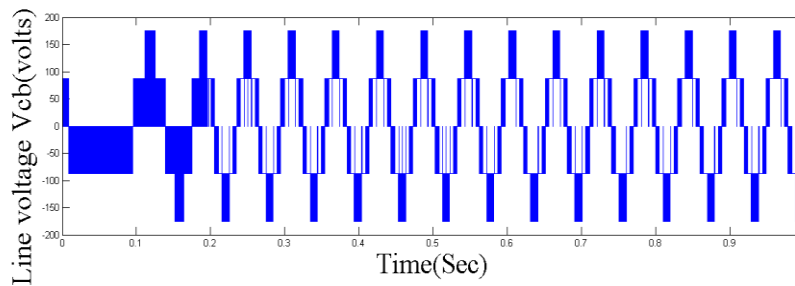**Fig. 9. Simulated value of line voltage $V_{ac}$ in (volts).**
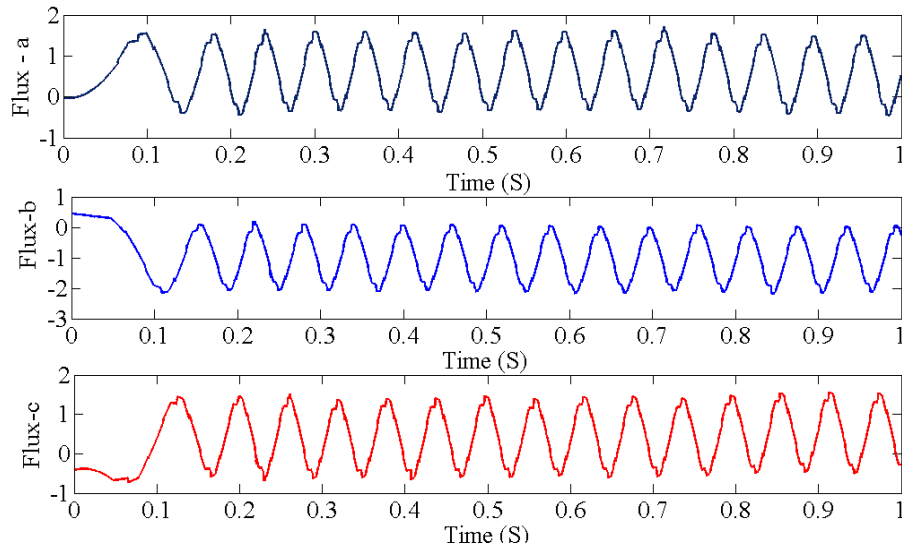


**Fig. 10. Simulated value of line voltage $V_{cb}$ (volts).**

**Fig. 11. Simulation results of flux linkages for 3-phases $\psi_a, \psi_b, \psi_c$ in webers.**
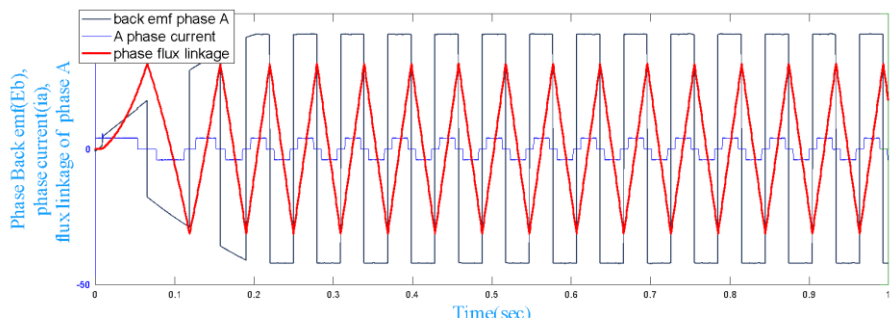


**Fig. 12. Back emf $E_b$ ( in volts), Current passing in phase A (amps), flux linkages in webers.**
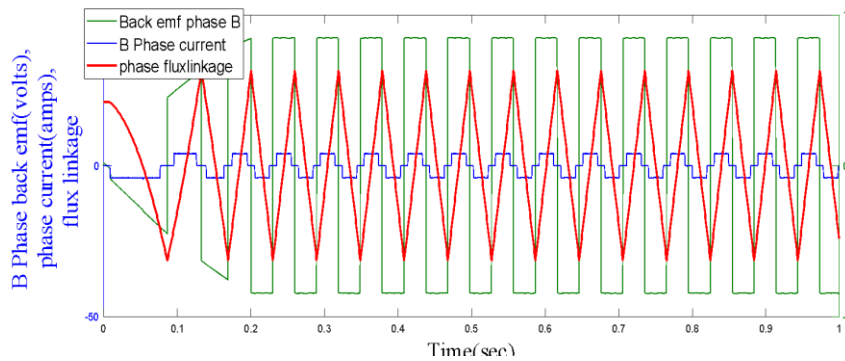


**Fig. 13. Back emf $E_b$ (volts), current passing in phase B (amps), flux linkages in webers.**
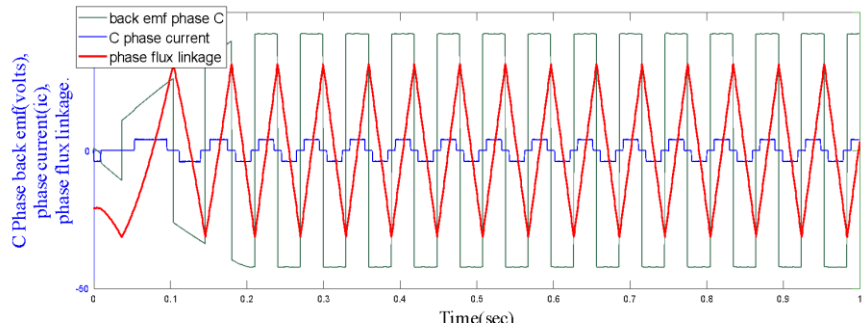
**Fig. 14. Back emf $E_b$ (volts), currents
passing in phase C(amps),flux linkage in (web).**

For the PI Controller, P gain of 1.4 and I gain of 15 are taken in order to get minimum ripples in the $V_{ref.}$. The design specifications of the DC-DC converter are given in Table A-2 (*Appendix A*). Speed response curve and its sudden dip in speed at 3rd second after the motor started is observed in Fig. 15. Electromagnetic torque with load variation shown in Fig.16. The computer based algorithm flow chart is shown in Fig. A-2 (*Appendix A*).
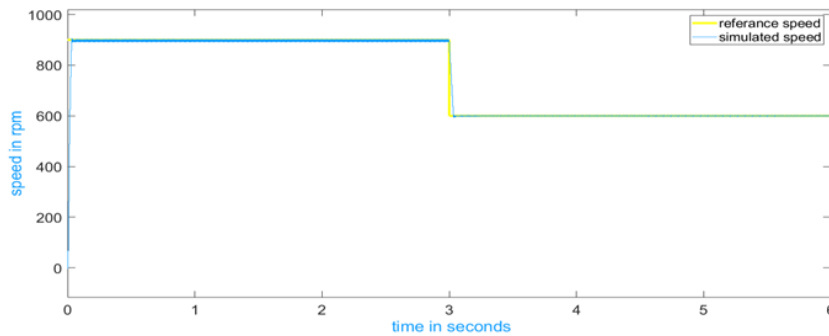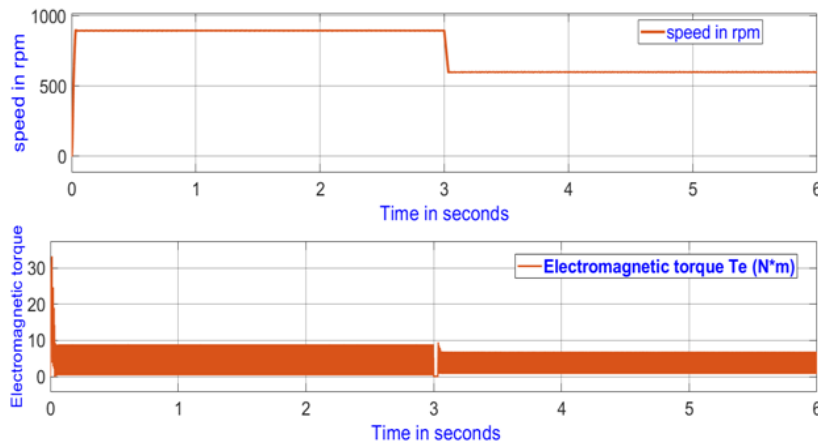


**Fig. 15. Motor speed in rpm vs time in seconds.**



**Fig. 16. Simulation value of electromagnetic torque (N.m).**

## 5. Conclusions

Zero crossing instant of Back emf on floating phase is the most popular sensorless controlling techniques among all the sensorless controlling techniques for BLDC drives. The back emf would be defined as $E_b = k.\omega$. In this expression the back emf is a speed dependent variable. Drawback of this back emf dependent techniques is, it cannot give accurate zero crossing instant during the motor at low speed or at standstill position. It may result in wrong switching patterns. The proposed technique overcomes this drawback and gives an accurate switching pattern for 3-phase BLDC motor for industrial usages.

● Align and go method for starting the BLDC here any two of Three phases excited using a very small amount of power. Very small amount of flux develops inside the machine, this flux is enough for prediction of the next rotor position of the motor. The small amount of flux (0.5 m- web) developed inside the machine. All required functions can be easily modified and extended through the simple software programme using the TMS320F28335 controller. In addition to the advantage of this new proposed flux linkage based sensorless method, The Integrated Buck Boost Buck converter serves as a strong front end converter. This converter can provide a high stable and constant boosted voltage at DC input side compared to conventional DC to DC converters.

● IB$^3$ converter also helps to minimise torque ripples on the motor side by continuously boosting the DC link voltages from primary side. Flux linkage based controlling technique is easy to implement, the speed of the motor varies automatically according to load variation during closed loop operation, the auto tuning method of the pi controller reduces the complexity of conventional tuning method. This technique can be implemented for EV applications, lifts and hoists, and industrial applications.

● Unlike the other sensorless controlling techniques this method gives better results, can be worked accurately even at continuous temperature changing work environments.

| **Nomenclatures** | |
| --- | --- |
| $C_0$ | Output filter capacitor in farads |
| $Cr$ | Bus capacitor in farads |
| $E_{ac}$, $E_{bc}$, $E_{ba}$ | Back emf's induced between two phases |
| $E_b$ | Back emf in volts. |
| $I_a.$, $I_b.$, $I_c.$ | currents passing in 3-phase windings |
| $K$ | Speed constant |
| $K_p$, $K_I$ | Proportional, Integral constants |
| $K_v$, $K_t$, $K_m$ | Velocity, torque, inertia constants |
| $L_0$ | Output inductance in henrys |
| $L_{as} + L_m = L$ | inductance at circuit balanced condition |
| $L_{as}$, $L_{bs}$, $L_{cs}$ | self-inductance in milli – henry |
| $Lr$ | Input inductance, in milli-henrys |
| $R_a = R_b =$ | Resistances of each phase in ohm's |
| $R_c = R$ | |
| $T_e$ | electromagnetic Torque |
| $T_L$ | Load torque |
| $V_a.$, $V_b.$, $V_c$ | Voltage difference between any phases to neutral. |

| $V_{ac}, V_{bc}, V_{ba}$ | Phase to phase voltage or line voltages |

**Greek Symbols**

| $\Phi$ | Phase lux linkages, webers |
| $\psi$ | Flux linkages, webers |
| $\omega_r$ | angular speed of rotor |

**Abbreviations**

| ADC | Analog- to- digital converter |
| BLDC | Brush less DC motor |
| DSP | Digital signal processor |
| EV | Electric vehicles. |
| FPGA | Field- programmable gate array |
| $IB^3$ | Integrated buck boost buck converter |
| IGBT | Integrated bipolar Transistor |
| KCL | Kirchhoff's current law |
| PI | Proportional Integral |
| PWM | Pulse width modulation |
| S1 to S6 | Switches(IGBT inverter switches) |
| SCR | Silicon controlled rectifier |
| s | Is a Laplace function |
| VSI | Voltage source inverter |

## References

1. Gamazo-Real, J.C.; Vázquez-Sánchez, E.; and Gómez-Gil, J. (2010). Position and speed control of brushless DC motors using sensorless techniques and application trends. *Sensors*, 10(7), 6901-6947.

2. Johnson, J.P.; Ehsani, M.; and Giizelgiinler, Y. (1999). Review of sensorless methods for brushless DC. *Conference Record of the* 1999 *IEEE Industry Applications Conference. Thirty-Fourth IAS Annual Meeting* (*Cat. No.99CH36370*), Phoenix, AZ, USA, 0197-2618.

3. Damodharan, P.; and Vasudevan, K. (2005). Indirect back-EMF zero crossing detection for sensorless BLDC motor operation. *International Conference on Power Electronics and Drives Systems* (*PEDS*), Kuala Lumpur, Malaysia, 1107-1111.

4. Cui, C.; Liu, G.; Wang, K.; and Song, X. (2015). Sensorless drive for high speed brushless DC motor based on the virtual neutral voltage. *IEEE Transactions on Power Electronics*, 30(6), 3275-3285.

5. Jang, G.H.; Park, J.H.; and Chang, J.H. (2002). Position detection and start-up algorithm of a rotor in a sensorless BLDC motor utilising inductance variation. *IEE Proceedings - Electric Power Applications*, 149(2), 137-142.

6. Singh, B.; and Singh, S. (2009). State of art on permanent magnet brushless Dc motor drives. *Journal of Power Electronics*, 9(1), 1-17.

7. Biswas, P.C.; and Ghosh, B.C. (2017). A novel flux estimation algorithm based position sensorless field oriented vector controlled permanent magnet brushless DC motor drive. 2017 3*rd International Conference on Electrical Information and Communication Technology* (*EICT*), Khulna, Bangladesh, 1-6.

8. Kim, T.-H.; and Ehsani, M. (2004). Sensorless control of the BLDC motors from near-zero to high speeds. *IEEE Transactions on Power Electronics*, 19(6), 1635-1645.

9. Matsui, N. (1996). Sensorless PM brushless dc motor drive. *IEEE Transactions on industrial Electronics*, 43(2), 300-308.

10. Nalli, R.; Subbarao, K.; Ramamoorthy, M.; and Kumar, M.K. (2019). Sensorless control of BLDC motor using flux linkage based algorithm. *International Journal of Engineering and Advanced Technology* (*IJEAT*), 8(6), 1549-1556.

11. Nagi, R.B.; Sekhar, O.C.; and Ramamoorty, M. (2019). Implementation of zero-current switch turn-On based buck-boost buck type rectifier for low power applications. *International Journal of Electronics*, 106(8), 1164-1183.

12. Nagi, R.B.; Sekhar, O.C.; and Ramamoorty, M. (2018). Analysis and implementation of single-stage buck-boost buck converter for battery charging applications. *Journal of Advanced Research in Dynamical and Control Systems*, 10(4). 446-457.

13. Sivani, L.S.; Nagi, R.B.; Rao, K.S.; and Alagappan, P. (2019). A new single switch AC/DC converter with extended voltage conversion ratio for SMPS applications. *International Journal of Innovative Technology and Exploring Engineering*, 8(3), 68-72.

14. Nagi, R.B.; Alagappan, P.; Sekhar, O.C.; and Ramamoorty, M. (2019). Performance and dynamic analysis of single switch AC-DC Buck-boost buck converter. *International Journal of Innovative Technology and Exploring Engineering*, 8(4), 307-313.

15. Ahmad, F.; Pandey, M.; and Zaid, M. (2018). Sensorless control of brushless dc motor by zero crossing detection  generation with adaptive power factor control technique, 2018 *IEEE International Conference on Environment and Electrical Engineering and* 2018 *IEEE Industrial and Commercial Power Systems Europe* (*EEEIC / I&CPS Europe*), Palermo, Italy, 1-6.

16. Awchar, S.M.; Diwan, S.P.; and Arlikar, P. (2018). Advanced technique for speed control of sensorless BLDC motor. 2018 *Fourth International Conference on Computing Communication Control and Automation* (*ICCUBEA*), Pune, India, 1-5.

17. Sajid, A.B.; Marryam, A.; and Ali, M. (2021), Modelling and control of Brushless DC motor. *Easy Chair Preprint*, 1-9.

18. TMS320F2833x.; TMS320F2823x. (2021). Digital signal controllers (DSCs) from Texas Instruments revised

19. Rambabu, S. (2007). Modeling and control of a brushless DC motor. M.Sc. Thesis, National Institute of Technology, NIT Rourkela.

## *Appendix A*

## Computer Programme

### A.1. Introduction

The Xilinx programming software is used as interfacing between computer language and embedded firmware.

### A.2. Flow Chart Structure

Flow chart structure is designed using Microsoft Visio application for clear sketch of flow chart.

**Table A-1. BLDC Motor designed specifications.**

| Name of the parameter | Rated Value |
|---|---|
| Inductance /phase, $L$ | 9.4 mH |
| Coefficient of damping, $B$ | 0.005N-m/rad/s |
| Load torque, $Tl$ | 12.5 Nm |
| Rated phase current, $A$ | 5 A. |
| Resistance/ phase, $R$ | 1.43 Ω |
| Number of poles, $P$ | 4 |
| Rated magnitude of voltage, $V$ | 200 V |
| Inertia constant, $J$ | 0.00208 kg.m$^2$ |

**Table A-2. Design specifications of (IB$^3$) Dc-Dc Converter. (Refer to Fig. 1).**

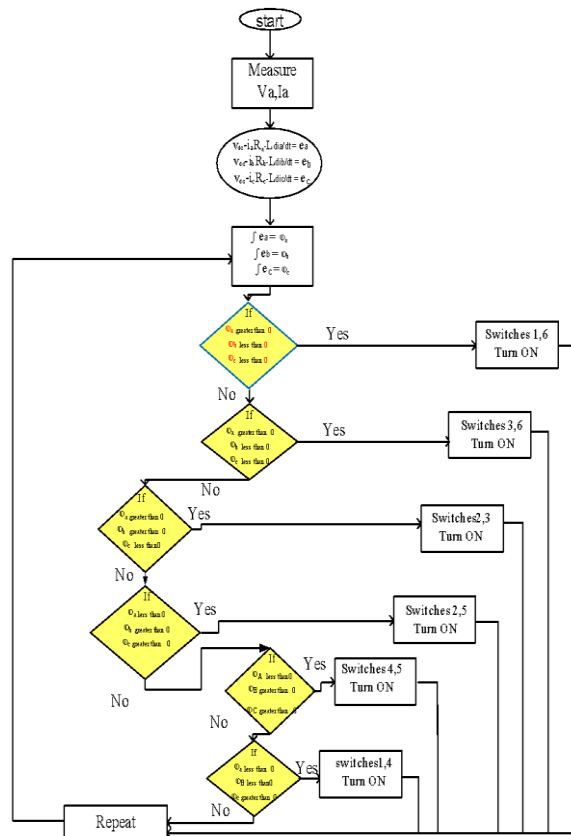| Parameter | Simulation |
|---|---|
| Input Voltage | 230V |
| Max Output Voltage | 350V |
| Max. Power | 1KW |
| Filter Inductor | 3mH |
| Filter Capacitor | 0.02uF |
| Supply Line Frequency($f_l$) | 50 Hz |
| Switching Frequency ( $f_s$ ) | 50 kHz |
| Input inductance, $L_r$ | 176uH |
| Bus capacitor, $C_r$ | 330uF |
| Output inductance, $L_0$ | 0.3mH |
| Output filter capacitor, $C_0$ | 500uF |



**Fig. A-1. Flow chart of the proposed sensorless controlling technique algorithm.**